

14-3-3 cooperates with LKB1 to regulate the activity and localization of QSK and SIK

Abdallah K. Al-Hakim^{1,*}, Olga Göransson¹, Maria Deak¹, Rachel Toth¹, David G. Campbell¹, Nick A. Morrice¹, Alan R. Prescott² and Dario R. Alessi¹

¹MRC Protein Phosphorylation Unit, MSI/WTB complex, University of Dundee, Dow Street, Dundee, DD1 5EH, UK

²Division of Cell Biology and Immunology, MSI/WTB complex, University of Dundee, Dow Street, Dundee, DD1 5EH, UK

*Author for correspondence (e-mail: a.alhakim@dundee.ac.uk)

Accepted 31 August 2005

Journal of Cell Science 118, 5661-5673 Published by The Company of Biologists 2005

doi:10.1242/jcs.02670

Summary

The LKB1 tumour suppressor kinase phosphorylates and activates a number of protein kinases belonging to the AMP-activated protein kinase (AMPK) subfamily. We have used a modified tandem affinity purification strategy to identify proteins that interact with AMPK α , as well as the twelve AMPK-related kinases that are activated by LKB1. The AMPK β and AMPK γ regulatory subunits were associated with AMPK α , but not with any of the AMPK-related kinases, explaining why AMP does not influence the activity of these enzymes. In addition, we identified novel binding partners that interacted with one or more of the AMPK subfamily enzymes, including fat facets/ubiquitin specific protease-9 (USP9), AAA-ATPase-p97, adenine nucleotide translocase, protein phosphatase 2A holoenzyme and isoforms of the phospho-protein binding adaptor 14-3-3. Interestingly, the 14-3-3 isoforms bound directly to the T-loop Thr residue of QSK and SIK, after these were phosphorylated by LKB1. Consistent with this, the 14-3-3 isoforms failed to interact with non-

phosphorylated QSK and SIK, in LKB1 knockout muscle or in HeLa cells in which LKB1 is not expressed. Moreover, mutation of the T-loop Thr phosphorylated by LKB1, prevented QSK and SIK from interacting with 14-3-3 in vitro. Binding of 14-3-3 to QSK and SIK, enhanced catalytic activity towards the TORC2 protein and the AMARA peptide, and was required for the cytoplasmic localization of SIK and for localization of QSK to punctate structures within the cytoplasm. To our knowledge, this study provides the first example of 14-3-3 binding directly to the T-loop of a protein kinase and influencing its catalytic activity and cellular localization.

Supplementary material available online at
<http://jcs.biologists.org/cgi/content/full/118/23/5661/DC1>

Key words: AMPK, MARK/Par1, Cell polarity, Mass spectrometry, Tandem affinity purification.

Introduction

The LKB1 protein kinase was originally identified as a gene mutated in the inherited Peutz Jeghers Syndrome (PJS), in which subjects are predisposed to developing benign and malignant tumours (Hemminki et al., 1998; Jenne et al., 1998). Subsequent work indicated that LKB1 forms a complex with the regulatory proteins STRAD and MO25 (Baas et al., 2003; Boudeau et al., 2003), and is likely to function as a tumour suppressor by regulating cell proliferation and polarity (reviewed by Baas et al., 2004). The first identified physiological substrate of LKB1 was the AMP-activated protein kinase (AMPK) (Hawley et al., 2003; Shaw et al., 2004b; Woods et al., 2003), which functions as a regulator of cellular energy (Hardie, 2004). LKB1 activates AMPK by phosphorylating Thr172 in the T-loop of this enzyme. The two isoforms of AMPK (AMPK α 1 and AMPK α 2) are associated with AMPK β and AMPK γ regulatory subunits, enabling AMPK to be activated under low energy conditions by binding of 5'-AMP to the AMPK γ subunit (Hardie, 2004). The binding of AMPK to 5'-AMP also promotes the phosphorylation and activation of AMPK by the LKB1 complex. Tumour formation in LKB1-deficient cells could result from deregulation of pathways involving the tuberous sclerosis complex/mTOR

(Corradetti et al., 2004; Shaw et al., 2004a) or p53 (Jones et al., 2005), which are reportedly regulated by AMPK.

LKB1 also phosphorylates and activates at least 12 other protein kinases that are closely related to AMPK, namely QSK, SIK, QIK, MARK1, MARK2, MARK3/Par-1A/C-TAK1, MARK4, NUA1/ARK5, NUA2/SNARK, BRK1/SAD-A, BRK2/SAD-B and SNRK (Jaleel et al., 2005; Lizcano et al., 2004). The most studied of these enzymes are the MARK isoforms, which regulate anterior-posterior cell polarity development at the one-cell stage of embryonic development in *C. elegans* (Guo and Kemphues, 1995) and *Drosophila* (Shulman et al., 2000). The MARK enzymes also control gastrulation in *Xenopus* (Kusakabe and Nishida, 2004). In mammals, MARK isoforms phosphorylate Tau (Drewes et al., 1997), thereby priming it for hyperphosphorylation by the kinases GSK-3 and Cdk5, an event that induces the aggregation of Tau into the toxic filaments and tangles that are observed in patients with Alzheimer's disease (Nishimura et al., 2004). Recent studies employing mice lacking BRK1 and BRK2, which are exclusively expressed in the brain, indicate that these enzymes play a key role in regulating neuronal polarization (Kishi et al., 2005). Less is known regarding the function of other AMPK-related kinases, i.e. QSK, QIK, SIK,

NUAK1, NUAKE2 and SNRK. RNAi-mediated knockdown of QSK in *Drosophila* cells resulted in mitotic defects that included spindle and chromosome alignment abnormalities (Bettencourt-Dias et al., 2004). SIK (salt-inducible kinase), was first cloned from the adrenal glands of rats fed a high salt diet (Wang et al., 1999) and its mRNA is induced by membrane depolarization in the brain (Feldman et al., 2000). The mRNA expressing QIK (SIK2) is highest in adipose tissue and, in overexpression studies, QIK was reported to phosphorylate human IRS1 at the same residue phosphorylated by AMPK (Horike et al., 2003). QIK also phosphorylates the CREB co-activator TORC2, in unstimulated cells, to sequester it in the cell cytoplasm, thereby inhibiting CREB-dependent gene-expression (Screaton et al., 2004). In overexpression studies, NUAKE1 (ARK5) suppressed apoptosis induced by certain stimuli, including nutrient starvation (Suzuki et al., 2003a), and was also suggested to regulate Caspase-6 activity (Suzuki et al., 2004b). NUAKE2 (SNARK) was shown to be most highly expressed in the kidney, and its activity was reportedly stimulated by glucose starvation of cells (Lefebvre et al., 2001; Suzuki et al., 2003b). Expression of NUAKE2 was also upregulated by CD95 and TNF in apoptosis-resistant tumour cell lines, and it plays a role in protecting these cells from apoptosis (Legembre et al., 2004). SNRK mRNA was induced threefold when granule neurons were cultured in low potassium, indicating that it could play a role in regulating survival responses in these cells (Yoshida et al., 2000). SNRK is also highly expressed in testis (Jaleel et al., 2005).

To date, little is known regarding the mechanism of regulation of AMPK-related kinases. Our analysis has indicated that none of the AMPK-related kinases is activated by agonists that stimulate AMPK, such as AICA-riboside or phenformin, or by muscle contraction (Lizcano et al., 2004; Sakamoto et al., 2004). However, it has also been reported that the AICA-riboside AMP mimetic, activated NUAKE2 in a hepatocarcinoma-derived cell line, suggesting that NUAKE2-like AMPK possesses an AMP-binding subunit (Lefebvre and Rosen, 2005).

In order to determine whether any of the AMPK-related kinases were complexed to AMPK β and AMPK γ regulatory subunits or associated with other binding partners, we have performed a tandem affinity purification analysis with each of the LKB1-activated AMPK-related kinases. Our findings indicate that the 14-3-3 phospho-protein binding adaptors (Mackintosh, 2004) cooperate with LKB1 to regulate the activity and localization of QSK and SIK.

Materials and Methods

Materials

Protein G-Sepharose, calmodulin-Sepharose 4B, glutathione-Sepharose, streptavidin-Sepharose, [γ - 32 P]ATP and enhanced chemiluminescence reagent were purchased from Amersham Bioscience; protease-inhibitor cocktail tablets, and precast SDS polyacrylamide Bis-Tris gels were from Invitrogen; Tween-20, rabbit IgG-agarose and dimethyl pimelimidate were from Sigma; NP-40 was from Fluka; and phosphocellulose P81 paper was from Whatman. The hexahistidine-tagged TEV protease was expressed in *E. coli* by G. Kular and purified using nickel agarose affinity chromatography and gel filtration. All peptides were synthesized by Graham Bloomberg at the University of Bristol.

Antibodies

The following antibodies were raised in sheep and affinity purified on the appropriate antigen: anti-LKB1 (raised against mouse protein, used for immunoblotting), anti-QSK (residues 1349-1369 of human QSK, TDILLSYKHPEVSFSMEQAGV, used for immunoblotting and immunoprecipitation), Phospho-anti-T-loop QSK/SIK (residues 175-189 of human SIK, KSGEPLST(P)WCGSPPY phosphorylated at Thr183, used for immunoblotting), anti-SIK (residues 1-20 of human SIK, MVIMSEFSADPAGQGQQQK, used for immunoblotting and immunoprecipitation), Phospho-anti-T-loop MARK (residues 204-218 of human MARK3 phosphorylated at Thr211, TVGGKLDTP)FCGSPPY, used for immunoblotting) and the anti-GST (raised against the glutathione S-transferase protein, used for immunoblotting). Anti-MARK3 antibody used for immunoblotting was from Upstate Biotech (anti c-TAK #05-680), polyclonal antibody recognizing 14-3-3 isoforms used for immunoblotting was purchased from Santa Cruz (#sc629), mouse monoclonal [4D11] recognizing the hexahistidine affinity tag were from Abcam (#ab5000-100), monoclonal antibodies recognizing HA epitope tag was purchased from Roche (#1666606), and secondary antibodies coupled to horseradish peroxidase used for immunoblotting were obtained from Pierce.

General methods

Tissue culture, transfection, immunoblotting, restriction enzyme digests, DNA ligations, and other recombinant DNA procedures were performed using standard protocols. All mutagenesis was carried out using the Quick-Change site-directed mutagenesis method (Stratagene). DNA constructs used for transfection were purified from *E. coli* DH5 α using Qiagen plasmid Mega or Maxi kit according to the manufacturer's protocol. All DNA constructs were verified by DNA sequencing, which was performed by The Sequencing Service, School of Life Sciences, University of Dundee, UK, using DYEnamic ET terminator chemistry (Amersham Biosciences) on Applied Biosystems automated DNA sequencers. The generation and culture of HeLa cells stably expressing wild-type or kinase-inactive LKB1[D179A] has been described previously (Sapkota et al., 2002).

Buffers

Lysis buffer contained: 50 mM Tris-HCl pH 7.5, 1 mM EGTA, 1 mM EDTA, 1% (w/v) NP-40, 1 mM sodium orthovanadate, 10 mM sodium- β -glycerophosphate, 50 mM sodium fluoride, 5 mM sodium pyrophosphate, 0.27 M sucrose, 1 mM dithiothreitol (DTT) and complete proteinase inhibitor cocktail (one tablet/50 ml). Buffer A contained: 50 mM Tris/HCl pH 7.5, 0.1 mM EGTA, 0.27 M sucrose and 1 mM DTT. Buffer B contained: 50 mM Tris-HCl pH 7.5, 0.15 M NaCl, 0.27 M sucrose, 1% (w/v) NP-40 and 1 mM DTT. Buffer C contained: 50 mM Tris pH 7.5, 0.15 M NaCl, 1 mM MgCl $_2$, 1 mM imidazole, 2 mM CaCl $_2$, 0.27 M sucrose and 1 mM DTT. Buffer D contained: 10 mM Tris pH 7.5, 1 mM imidazole, 20 mM EGTA, and 1 mM DTT. TBS-Tween buffer contained: 50 mM Tris/HCl pH 7.5, 0.15 M NaCl and 0.2% (v/v) Tween-20.

Plasmids

The generation of wild-type and mutant epitope-tagged AMPK-related kinases in the pEBG2T vector encoding for the expression of GST-fusion proteins in eukaryotic cells have been described previously (Lizcano et al., 2004). The wild-type and mutant QSK were subcloned into the pEGFP-C1 vector (Clontech) as a *Bam*HI-*Bam*HI fragment from the pEBG2T vector. The wild-type and mutant SIK were subcloned into *Not*I-modified pEGFP-C1 vector as *Bam*HI-*Not*I fragment from pEBG2T vector. A cDNA of full-length N-terminally Myc-tagged rat AMPK α 1[T172E], was kindly provided by G. Hardie, and subcloned into the *Eco*RI-*Kpn*I sites of the pEGFP-

C2-TAP vector. 14-3-3 ζ (GenBank NM_145690) was amplified from IMAGE EST clone 2988020 with oligonucleotides introducing a *Bam*HI restriction site at both the 5' and 3' ends and was subcloned into a pGEX6P-1 vector. TORC2 (GenBank NM_181715) was amplified from IMAGE EST clone 6188068 with oligonucleotides introducing a *Not*I restriction site at both the 5' and 3' ends and subcloned into pGEX6P-2 vector. The kinase-inactive SIK[D167A], T-loop mutant SIK[T182A], kinase inactive QSK[D206A] and T-loop mutant QSK[T221A] have been described previously (Lizcano et al., 2004).

Generation of the pEBGFP-C2-TAP vector

Based on the original Tandem Affinity Purification strategy (Rigaut et al., 1999), we constructed a modified expression vector described in Fig. 1A that incorporates a green fluorescent protein (GFP) tag before the TAP tag to enable more facile selection of stable cell lines that express TAP-tagged proteins. In addition we have also inserted an additional precision protease cleavage site immediately after the calmodulin binding motif to enable cleavage of the TAP-tagged protein from the calmodulin-Sepahrose without using EDTA or SDS elution methods and to permit removal of the entire tag of the expressed TAP-tagged protein after purification if necessary. To generate this vector we used a PCR based strategy employing as a

template a vector encoding two tandem protein A IgG-binding domains (IGG1 and IGG2) and a calmodulin-binding motif that was kindly provided by B. Seraphin (EMBL, Heidelberg, Germany) and modified by M. Stark (School of Life Sciences, Dundee). The primers used for this PCR (5'-gccaccatggacacaagtgccaccatgaagc-3' and 5'-gcgccgcgggtaccagatctggatcccagggggcccctggaacagaactccagagcagttggaatataatcaatgaagtgcgcc-3') incorporated a precision protease site and a *Bam*HI and *Not*I restriction enzyme site after the calmodulin-binding domain. The resulting PCR product was ligated into pCR2.1.TOPO vector (Invitrogen). This was then subcloned in-frame into the polylinker region of pEGFP-C2 vector as an *Eco*RI-*Eco*RI fragment. The upstream *Eco*RI site and the downstream *Bam*HI site in the polylinker region of the resulting vector were then eliminated by PCR mutagenesis. The resulting vector described in Fig. 1A is termed pEGFP-C2-TAP, and enables proteins to be tagged at their N-terminus with a GFP-TAP tag. The cloning of HA-epitope-tagged AMPK-related kinases has been described previously (Lizcano et al., 2004) and the full-length coding regions of these enzymes were appropriately subcloned as *Bam*HI-*Bam*HI, *Bam*HI/*Eco*RI, *Not*I/*Not*I or *Bam*HI-*Not*I fragments into the pEGFP-C2-TAP vector to incorporate an N-terminal GFP-TAG. Human 14-3-3 ζ was also subcloned in to the pEGFP-C2-TAP as a *Not*I-*Not*I fragment.

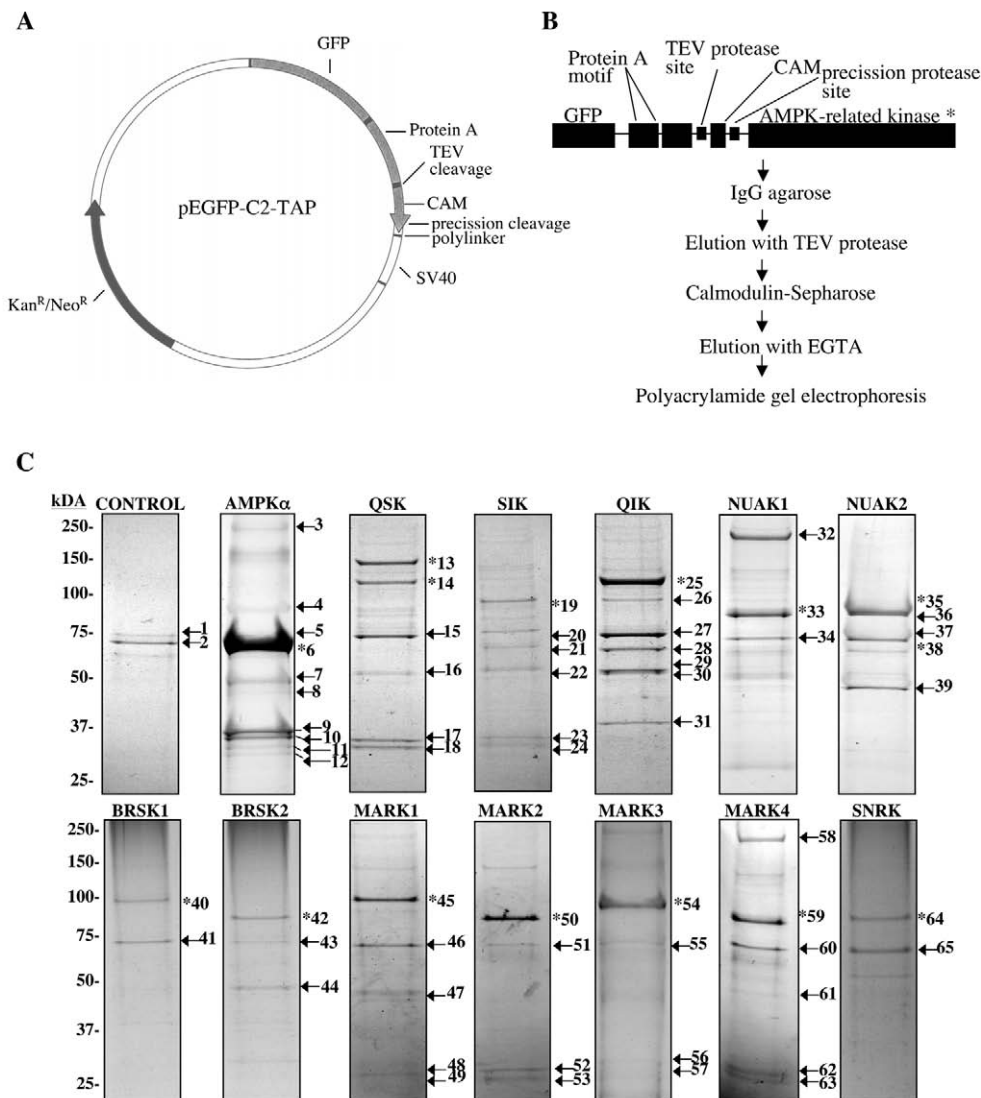


Fig. 1. TAP-purification of AMPK-related kinases. (A) The pEGFP-C2-TAP vector, depicting the affinity tag added to the N-terminus of AMPK α 1 and the AMPK-related kinases, consisting of a green fluorescent protein (GFP), protein A and a calmodulin-binding motif (CAM) flanked by TEV and precision protease cleavage sites, prior to multiple cloning sites. (B) Outline of the strategy that was employed to affinity purify the GFP-TAP-tagged kinases. (C) The TAP affinity purified kinases were electrophoresed on a polyacrylamide gel and the protein bands visualized following colloidal Coomassie Blue staining. Each of the major bands observed that we were able to identify by mass spectrometry was numbered and its identity indicated in Table 1. Bands that were not reliably identified are left unlabelled. *The bands identified as the bait kinase.

Generation of stable cell lines

HEK 293 cells were cultured in 10 cm diameter dishes to 50-70% confluence and transfected with 2 μg pEGFP-C2-TAP construct encoding rat AMPK α 1[T172E] or human full-length wild-type AMPK-related kinases using Fugene 6 reagent (Roche) according to the manufacturer's instructions. After 24 hours, G418 was added to the medium to a final concentration of 3 mg/ml, and the medium was changed every 24 hours maintaining G418. After 14-20 days, individual surviving colonies expressing low levels of GFP-fluorescence were selected and expanded. FACS analysis was also performed to ensure uniform expression of GFP in the selected cell lines and anti-HA immunoblotting analysis of lysed cells was performed to ensure that the expressed proteins migrated as a single molecular weight species at the expected apparent molecular mass (the isolated GFP-TAP tag adds 50 kDa to the molecular mass of a protein). For the TAP-purification, we selected the stable cell lines that expressed the low levels of GFP-TAP-AMPK-related kinases to maximize the proportion of purified enzyme that is bound to an endogenous binding partner. HeLa cells lacking LKB1 and those expressing wild-type LKB1 (Sapkota et al., 2002) were stably transfected with GFP-TAP-14-3-3 ζ using the same protocol as for 293 cells except that lipofectamine was used for the transfection.

Tandem affinity purification

The purification method was adapted from the previously described TAP-purification protocol (Rigaut et al., 1999). For each TAP-purification, we cultured fifty 15 cm dishes of confluent cell line. Each dish of cells was washed twice with ice-cold phosphate buffered saline and then lysed in 1.0 ml of ice-cold lysis buffer. The combined lysates were centrifuged at 26,000 g for 30 minutes at 4°C and the supernatant incubated with 0.4 ml of rabbit IgG-agarose beads for 1 hour at 4°C. The IgG-agarose was washed extensively with lysis buffer containing 0.15 M NaCl, and then with several washes in buffer B prior to incubation with 0.4 ml of buffer B containing 0.1 mg of TEV protease. After 3 hours at 4°C ~70-90% of the TAP-tagged AMPK-related kinase had been cleaved from the IgG-agarose and the eluted protein was incubated with 0.4 ml of rabbit calmodulin-Sepharose equilibrated in buffer C. After 1 hour at 4°C the calmodulin-Sepharose was washed with buffer C containing 0.1% (v/v) NP-40 followed by a final wash with buffer C containing 10 mM Tris pH 7.5, no NaCl, no sucrose and 0.02% (v/v) NP-40. The calmodulin-Sepharose was then incubated with 1 ml buffer D. The resin was also washed with 0.4 ml of 0.05 \times NUPAGE-LDS sample buffer [6.8 mM Tris 0.1% (w/v) LDS (lithium dodecyl sulphate), 0.5% (v/v) glycerol containing 1 mM DTT final pH 8.5]. The two eluates were kept separately and concentrated by speed vac to 0.1 ml. The EGTA-eluted sample was added to 40 μl of NUPAGE-LDS sample buffer [purchased from Invitrogen containing 0.55 M Tris 8% (w/v) LDS (lithium dodecyl sulphate), 40% (v/v) glycerol containing 10 mM DTT final pH 8.5] and the resulting solution heated for 5 minutes at 70°C and allowed to cool to room temperature. For both eluates, iodoacetamide was added to 50 mM in order to alkylate Cys residues. After incubation in the dark for 30 minutes at room temperature, DTT was added to a final concentration of 0.1 M and 45 μl of each sample was electrophoresed on a precast 4-12% SDS-polyacrylamide gel, which was then stained with colloidal Coomassie Blue and photographed. The bands indicated in Fig. 1C for each of the AMPK-related kinase purifications were excised, washed and digested with trypsin as described previously (Woods et al., 2001). Peptides were analysed by combined MALDI-TOF, MALDI-TOF/TOF MS (matrix-assisted laser-desorption ionization-time-of-flight/time of flight mass spectrometry) analysis on an Applied Biosystems 4700 ToF/ToF Proteomics Analyser using 5 mg/ml α -cyano cinnamic acid in 10 mM ammonium phosphate as the matrix or by LC-MS on an Applied Biosystems 4000 Q-TRAP. The Celeris Discovery System (Applied

Biosystems) human database was searched using the Mascot search algorithm [http://www.matrixscience.com (Perkins et al., 1999)].

Expression and purification of 14-3-3 ζ and TORC2 in *E. coli*

The pGEX expression constructs encoding human wild-type or mutant [K180E] 14-3-3 ζ as well as wild-type human TORC2 were transformed into *E. coli* BL21 cells. One-litre cultures were grown at 37°C in Luria broth containing 100 $\mu\text{g}/\text{ml}$ ampicillin until the absorbance at 600 nm was 0.8. Induction of protein expression was carried out by adding 100 μM isopropyl-B-D-galactoside and the cells were cultured for a further 16 hours at 26°C. Cells were isolated by centrifugation, resuspended in 15 ml of ice-cold lysis buffer and lysed in one round of freeze/thawing, followed by sonication to fragment DNA. The lysates were centrifuged at 4°C for 30 minutes at 26,000 g , and the recombinant proteins were affinity purified on glutathione-Sepharose and eluted in buffer A containing 20 mM glutathione.

Expression and purification of AMPK-related kinases in 293 cells

Five 10 cm diameter dishes of HEK 293 cells were cultured and each dish transfected with 10 μg of the pEBG-2T construct encoding wild-type or indicated mutant forms of AMPK-related kinase using the polyethylenimine method (Durocher et al., 2002). The cells were cultured for a further 36 hours and lysed in 0.5 ml of ice-cold lysis buffer, the lysates pooled and centrifuged at 4°C for 10 minutes at 26,000 g . The GST-fusion proteins were purified by affinity chromatography on glutathione-Sepharose and eluted in buffer A containing 20 mM glutathione.

Immunoblotting

Total cell lysate (10-50 μg) or immunoprecipitated samples were heated at 70°C for 5 minutes in SDS sample buffer, and subjected to polyacrylamide gel electrophoresis and electrotransfer to nitrocellulose membrane. Membranes were blocked for 1 hour in TBS-Tween buffer containing 10% (w/v) skimmed milk. The membranes were probed with 1 $\mu\text{g}/\text{ml}$ of indicated antibodies in TBS-Tween, 5% (w/v) skimmed milk for 16 hours at 4°C. Detection was performed using horseradish peroxidase-conjugated secondary antibodies and the enhanced chemiluminescence reagent.

Measurement of AMPK-related kinase catalytic activity

The activity of purified AMPK-related kinases was quantified by measurement of phosphorylation of the AMARA (AMARAASAAALRRR) peptide substrate (Lizcano et al., 2004) or the CREB co-activator TORC2 protein substrate (Screaton et al., 2004). For the kinase activity assay using AMARA peptide as a substrate, 10-100 ng AMPK-related kinase was incubated in a 50 μl mixture containing 50 mM Tris-HCl pH 7.5, 0.1% (v/v) 2-mercaptoethanol, 10 mM MgCl₂, 0.1 mM EGTA, 0.1 mM [γ -³²P]ATP (300 cpm/pmol) and 200 μM AMARA peptide for 20 minutes at 30°C. Incorporation of ³²P-phosphate into the peptide substrate was determined by applying 40 μl of the reaction mixture onto P81 phosphocellulose paper followed by scintillation counting after washing the papers in phosphoric acid as described previously. One unit (U) of activity was defined as that which catalysed the incorporation of 1 nmol of ³²P into the substrate. For the TORC2 protein substrate assay, 25 ng QSK or SIK was incubated for 20 minutes at 30°C in a volume of 30 μl containing 50 mM Tris-HCl pH 7.5, 0.1% (v/v) 2-mercaptoethanol, 10 mM MgCl₂, 0.1 mM EGTA, 0.1 mM [γ -³²P]ATP (300 cpm/pmol) and 2 μg GST-TORC2 peptide. Following polyacrylamide gel electrophoresis and Coomassie staining, the GST-TORC2 bands were excised and the incorporation of ³²P-phosphate, was determined by Cerenkov counting.

Immunoprecipitation of endogenous QSK and SIK

Quadriceps mouse muscle was isolated and homogenized as described previously (Sakamoto et al., 2005). HeLa cells were grown to confluence on 10 cm diameter dishes and lysed in 1 ml of lysis buffer. The QSK and SIK antibodies were covalently coupled to protein G-Sepharose in a ratio of 1 mg antibody to 1 ml resin using a dimethyl pimelimidate cross-linking procedure. Clarified quadriceps muscle extract or HeLa cell extract containing 1 mg total cell protein, were incubated at 4°C for 1 hour on a vibrating platform with 5 µl of the QSK or SIK-antibody-protein G-Sepharose conjugate. The immunoprecipitates were washed twice with 1 ml of lysis buffer containing 0.15 M NaCl and twice with 1 ml of buffer A. The immunoprecipitates were either subjected to protein kinase activity assay as described above or analysed by immunoblotting. Prior to immunoblotting the beads were washed in buffer A lacking DTT and resuspended in a volume of 20 µl of buffer A lacking DTT to which 5 µl of SDS sample buffer lacking DTT was added. The samples were subjected to electrophoresis and then immunoblotted as described above.

Affinity purification of 14-3-3 binding proteins

Clarified lysates of 293 cells containing 1 mg total cell protein, were incubated at 4°C for 1 hour on a vibrating platform with 20 µl glutathione-Sepharose conjugated to 20 µg GST-14-3-3ζ expressed in *E. coli* as described above. The beads were washed twice with 1 ml of lysis buffer containing 0.15 M NaCl, twice with 1 ml of buffer A and then subjected to electrophoresis and immunoblotting as described above.

Affinity purification of 14-3-3 isoforms with QSK T-loop peptide

293 cell lysate (3 mg protein) was incubated for 30 minutes at 4°C with 10 µg N-terminal Biotin-conjugated QSK-Phospho-T-loop peptide TPGQLIKT(P)WCGSPPY or QSK-T-loop peptide TPGQLIKTWCGSPPY. 10 µl Streptavidin-Sepharose, previously equilibrated in lysis buffer, was added to the lysates that were then incubated for another 1 hour on a vibrating platform at 4°C. The beads were washed twice with 1 ml lysis buffer containing 0.15 M NaCl, twice with 1 ml buffer A and then resuspended in a volume of 20 µl of buffer A to which 5 µl of SDS sample buffer was added. The samples were then subjected to electrophoresis and immunoblotted for 14-3-3 as described above.

Dissociation of 14-3-3 isoforms from QSK and SIK

GST fusion proteins of QSK and SIK were expressed in 293 cells and absorbed onto glutathione-Sepharose and washed with buffer A as described above. Aliquots of 20 µl of glutathione-Sepharose, still conjugated to GST-QSK or GST-SIK, were incubated with 200 µl of buffer A containing either no peptide or 10 µg of the QSK-Phospho-T-loop peptide (TPGQLIKT(P)WCGSPPY) or 10 µg of the QSK-T-loop peptide (TPGQLIKTWCGSPPY). After incubation for 30 minutes at 4°C on a vibrating platform, the beads were washed twice with 1 ml buffer A, and GST-SIK and GST-QSK was eluted in 20 µl buffer A containing 20 mM glutathione. Activity and immunoblotting analysis was performed on the eluted protein as described above.

14-3-3 overlay assay

Wild-type and T-loop mutant forms of GST-QSK, GST-SIK and wild-type GST-MARK3 (0.5 µg) were subjected to polyacrylamide gel electrophoresis and electrotransfer to nitrocellulose membrane. Overlay assays were undertaken using a previously described method (Moorhead et al., 1996). Briefly, membranes were blocked for 1 hour in TBS-Tween buffer containing 10% (w/v) skimmed milk and up to 0.5 M NaCl. The membranes were incubated with 5 µg/ml total His-BMH1 and His-BMH2 (yeast 14-3-3 isoforms), in TBS-Tween

containing 1 mg/ml BSA and up to 0.5 M NaCl for 16 hours at 4°C. The membranes were washed six times for 5 minutes with TBS-Tween containing up to 0.5 M NaCl. The membrane was probed with 1:5000 dilution of anti-His antibody in TBS-Tween, 5% (w/v) skimmed milk containing up to 0.5 M NaCl for 1 hour at room temperature. Detection was performed using horseradish-peroxidase-conjugated secondary antibodies and the enhanced chemiluminescence reagent.

Binding of 14-3-3ζ to peptides

1 µg of the indicated N-terminal biotin-linked peptides were conjugated for 15 minutes at 4°C with 5 µl of streptavidin-Sepharose, previously equilibrated in buffer A containing 0.2 mg/ml BSA. The beads were incubated with 100 ng or 300 ng of GST-14-3-3ζ purified from *E. coli* in a total volume of 0.1 ml in buffer A containing 0.2 mg/ml BSA, for 30 minutes at 4°C on a vibrating platform. The beads were washed twice with buffer A containing 0.15 M NaCl, twice with buffer A and then resuspended in a volume of 20 µl of buffer A to which 5 µl of SDS sample buffer was added. The samples were then subjected to electrophoresis and immunoblotted for 14-3-3 as described above.

Mapping SIK and QSK phosphorylation sites on TORC2

TORC2 (1 µg) was incubated for 10 minutes with 10 ng of GST-QSK or GST-SIK isolated from 293 cells that is associated with 14-3-3 or GST-QSK or GST-SIK from which 14-3-3 was dissociated as described. Phosphorylation reactions were performed in buffer A containing 5 mM Mg-acetate and 100 µM [γ -³²P]ATP (2500 cpm/pmol) in a total reaction volume of 25 µl. The reaction was terminated by adding SDS to a final concentration of 1% w/v and dithiothreitol to 10 mM and heated at 100°C for 1 minute. The sites phosphorylated on TORC2 were mapped after trypsin digestion and reverse phase HPLC, using an Applied Biosystems 4700 Proteomics Analyser (MALDI-TOF-TOF) and solid-phase Edman degradation on an Applied Biosystems 494C sequencer of the peptide coupled to Sequelon-AA membrane (Milligen) as described previously (Campbell and Morrice, 2002).

Localization studies

The different HeLa cell lines used in Fig. 5 were cultured to 50% confluence on glass coverslips (no. 1.5) in 60 mm diameter dishes and transfected with 0.4 µg of pEGFP construct encoding wild-type or indicated QSK or SIK mutants, using Fugene-6 transfection reagent (Roche) according to the manufacturer's protocol. A duplicate set of dishes was used for each condition. The cells were washed with PBS 20 hours post-transfection, and were fixed for 10 minutes in freshly prepared 3% (v/v) paraformaldehyde in PBS (Oxoid Limited, #BR0014G). The cells were then washed twice with PBS and permeabilized for 10 minutes with 1% (v/v) NP40 in PBS, followed by 1% (v/v) NP40 containing 0.5 µg/ml 4',6'-diamidino-2-phenylindole dihydrochloride (DAPI purchased from Fluka). The cells were viewed using a Zeiss LSM 510 META or Leica Sp2 AOBs confocal microscope.

Results

Identification of proteins that bind to AMPK α 1 and AMPK-related kinases

We generated human embryonic kidney 293 cell lines that stably express AMPK α 1 and 12 of the AMPK-related kinases that are activated by LKB1, each possessing a modified tandem affinity purification (TAP) tag (Puig et al., 2001; Rigaut et al., 1999) at their N-terminus that incorporates a GFP moiety (Fig. 1A). The presence of a GFP tag permits visual and FACS

sorting of stable cell lines that express low levels of the GFP-TAP-proteins, considerably facilitating the isolation/selection of these cells. The TAP tag also contains protein-A and calmodulin-binding motifs to permit facile purification of tagged proteins on IgG-agarose and calmodulin-Sepharose, respectively. We performed successive chromatography on agarose and Sepharose resins in order to prevent contamination of purified samples with Sepharose- or agarose-binding proteins. We selected stable cell lines in which the GFP-TAP-tagged fusion proteins were expressed in a non-proteolysed form and at as low as possible levels, as determined by immunoblot analysis of each of the selected stable cell lines. Each affinity purification was performed from fifty 15 cm diameter dishes of confluent cells, using the strategy outlined in Fig. 1B. The purified preparations were subjected to electrophoresis on a polyacrylamide gel, which was then stained with colloidal Coomassie Blue (Fig. 1C). The identity of the major colloidal Coomassie Blue-stained bands in each preparation was established by tryptic peptide mass-spectral fingerprinting procedures (Table 1).

In all samples, AMPK α 1 and the AMPK-related kinase baits were detected as the major staining band, migrating at their predicted molecular size (Fig. 1C). For QSK and NUA2, additional proteolysed forms of the bait were also detected. In

most samples, including the control cell line expressing only GFP-TAP, tubulin and Hsp70 were identified, which indicates that they were likely to comprise non-specific contaminants of our purification. Importantly, AMPK α 1 was found to be associated with its regulatory AMPK β 1, AMPK β 2 and AMPK γ 1 subunits (Fig. 1C, Table 1), thus validating this approach to identify physiological binding partners. By contrast, AMPK β and AMPK γ subunits were not associated with any of the AMPK-related kinases. Several other proteins were present at significant stoichiometry relative to the bait (Table 1). These included the 280 kDa fat facets/ubiquitin-specific protease 9 (USP9), which was associated with MARK4 and NUA1, the AAA-ATPase-p97, as well as the catalytic subunit of protein phosphatase 2A (PP2A) and its two regulatory A and B subunits that bound to QIK. NUA2 and AMPK α 1 were associated with a chaperone heterodimer consisting of Cdc37 and Hsp90, known to interact with numerous kinases, whereas the adenine nucleotide translocase bound AMPK α 1. The 14-3-3 ϵ and 14-3-3 ζ phospho-binding protein adapters (Mackintosh, 2004) were associated with QSK and SIK as well as with all four MARK isoforms.

We also undertook TAP purifications from stable cell lines expressing different levels of TAP-tagged MARK4 (supplementary material Fig. S1). 14-3-3 ζ , 14-3-3 ϵ and USP9

Table 1. Identification of proteins associated with AMPK-related kinases

Sample ID*	Protein	Sequence coverage (%)	Protein score [†]	Swiss-Prot acc. no.	Sample ID*	Protein	Sequence coverage (%)	Protein score [†]	Swiss-Prot acc. no.
1	GRP78	30	100	P11021	32	USP9	22	448	Q93008
2	Hsp70	35	140	P08107	33	Nuak1	48	409	O60285
3	Carbamoyl phosphate synthetase	10	691	Q6F8M7	34	Hsp70	20	52	P08107
4	Hsp90	28	741	P07900	35	Nuak2	24	192	Q9H093
5	Hsp70	14	262	P08107	36	Hsp90	22	221	P07900
6	AMPK α	43	1089	P54645	37	Hsp70	36	157	P08107
7	Tubulin	41	675	P05209	38	Nuak2	33	124	Q9H093
8	Cdc37	15	219	Q16543	39	cdc37	16	92	Q16543
9	AMPK β 1	47	300	Q9Y478	40	Brsk1	42	640	Q8TDC2
10	AMPK γ 1	43	391	P54619	41	Hsp70	57	389	P08107
11	AMPK β 2	51	385	O43741	42	Brsk2	52	397	Q81WQ3
12	Adenine nucleotide translocase 2	11	179	PO5141	43	Hsp70	39	256	P08107
13	Qsk	28	244	Q9Y2K2	44	Tubulin	32	147	P05209
14	Qsk	33	128	Q9Y2K2	45	Mark1	34	176	Q9POL2
15	Hsp70	37	248	P08107	46	Hsp70	33	111	P08107
16	Tubulin	28	96	P05209	47	Tubulin	32	98	P05209
17	14-3-3 ζ	40	178	P63104	48	14-3-3 ζ	25	83	P63104
18	14-3-3 ϵ	42	121	P62258	49	14-3-3 ϵ	34	140	P62258
19	SiK	19	127	Q86YJ2	50	Mark2	49	518	Q15524
20	Hsp70	37	131	P08107	51	Hsp70	42	120	P08107
21	SiK	25	116	Q86YJ2	52	14-3-3 ζ	25	83	P63104
22	Tubulin	34	119	P05209	53	14-3-3 ϵ	32	127	P62258
23	14-3-3 ζ	30	98	P63104	54	Mark3	34	178	P27448
24	14-3-3 ϵ	38	120	P62258	55	Hsp70	25	83	P08107
25	Qik	30	260	Q9H0K1	56	14-3-3 ζ	31	98	P63104
26	VCP	33	210	P55072	57	14-3-3 ϵ	34	104	P62258
27	Hsp70	52	369	P08107	58	USP9	14	204	Q93008
28	PP2A reg. subunit A	38	199	Q8NHV8	59	Mark4	56	565	Q96GZ3
29	Tubulin	24	98	P05209	60	Hsp70	25	122	P08107
30	PP2A reg. subunit B	49	145	P63151	61	Tubulin	25	98	P05209
31	PP2A catalytic subunit	49	203	P67775	62	14-3-3 ζ	35	104	P63104
					63	14-3-3 ϵ	36	120	P62258
					64	Snrk	11	91	Q9NRH2
					65	Hsp70	34	125	P08107

*The colloidal Coomassie-Blue-stained bands that were labelled as indicated in Fig. 1C were excised from the gel, digested in-gel with trypsin, and their identities were determined by tryptic peptide mass-spectral fingerprint as described in Materials and Methods.

[†]Mascot protein score where a value >63 is considered significant ($P < 0.05$).

were clearly associated with MARK4 derived from stable cell lines expressing a low and a five- to tenfold higher level of MARK4. Interestingly, however, MARK4 isolated from 293 cells expressing higher levels of MARK4 resulting from transient transfection, revealed the presence of only 14-3-3 isoforms associated with MARK4, but not USP9 (supplementary material Fig. S1).

Binding of QSK and SIK to 14-3-3 is LKB1-dependent

We next explored whether the interaction of AMPK-related kinases with 14-3-3 was regulated by LKB1. We have recently described the generation of mice that lack expression of LKB1 in skeletal muscle (Sakamoto et al., 2005). Strikingly, QSK immunoprecipitated from LKB1-knockout muscle was not

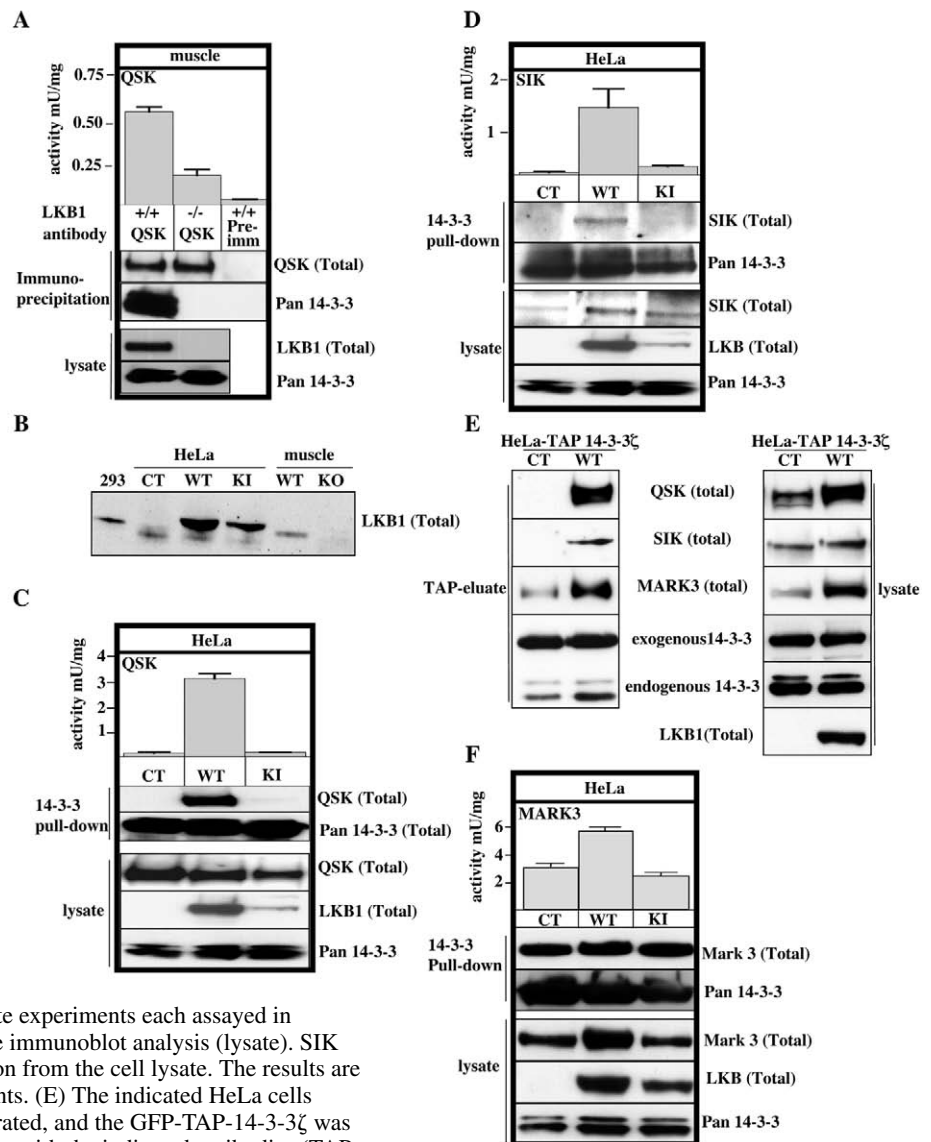
associated with 14-3-3, whereas QSK derived from wild-type muscle was bound to 14-3-3 (Fig. 2A). QSK was markedly less active in LKB1-deficient muscle, consistent with it not being phosphorylated at its T-loop. As SIK was not detected in mouse skeletal muscle (AKA, data not shown) we could not test whether it was associated with 14-3-3 in this system.

We next addressed whether AMPK-related kinases interacted with 14-3-3 isoforms in cell extracts derived from control HeLa cells that do not express LKB1 or HeLa cells stably expressing wild-type or kinase-inactive LKB1. As reported previously (Hawley et al., 2003; Lizcano et al., 2004), the kinase-inactive LKB1 is expressed at lower levels than wild-type LKB1 in the HeLa cell lines, but is still expressed at higher levels than endogenously expressed LKB1 in 293 cells or in mouse skeletal muscle (Fig. 2B). Cell extracts derived

Fig. 2. Binding of 14-3-3 to QSK and SIK, but not MARK3 is dependent on LKB1.

(A) QSK was immunoprecipitated from the quadriceps muscle derived from wild-type mice (LKB1^{+/+}) and muscle-specific LKB1-knockout (LKB1^{-/-}) mice (Sakamoto et al., 2005). As a control, immunoprecipitation from LKB1^{+/+} muscle was also performed with a preimmune antibody. The immunoprecipitates (IP) were subjected to immunoblot analysis and also assayed using the AMARA peptide. Muscle samples derived from five LKB1^{-/-} and LKB1^{+/+} mice were analysed and similar results obtained for each one. The QSK activity is the mean \pm s.d. for each muscle sample assayed in duplicate. Pre-imm, pre-immune antibody. (B) Cell lysates (20 μ g) derived from 293 cells, control (CT) HeLa cells that lack LKB1 expression, or HeLa cells that stably express wild-type (WT) or kinase-inactive (KI) LKB1, as well as skeletal muscle derived from wild-type (WT) and muscle-specific LKB1-knockout (KO) mice, were immunoblotted with an antibody recognizing LKB1. (C,D,F) Cell lysates derived from control (CT) HeLa cells that lack LKB1 expression or HeLa cells that stably express wild-type (WT) or kinase-inactive (KI) LKB1 were incubated with glutathione-Sepharose conjugated to 14-3-3 ζ (14-3-3 pull-down). After washing, the beads were immunoblotted with the indicated antibodies. The activity of the indicated AMPK-related kinases towards the AMARA peptide was also measured following immunoprecipitation. The results are presented as the mean \pm s.d. from two separate experiments each assayed in triplicate. Cell lysates were also subjected to the immunoblot analysis (lysate). SIK was immunoblotted after its immunoprecipitation from the cell lysate. The results are representative of at least two separate experiments. (E) The indicated HeLa cells stably expressing GFP-TAP-14-3-3 ζ were generated, and the GFP-TAP-14-3-3 ζ was affinity purified and analysed by immunoblotting with the indicated antibodies (TAP-eluate). Cell lysates derived from the HeLa cells were also immunoblotted (lysate).

As GFP-TAP-14-3-3 ζ migrates to the same position as endogenous MARK3, thereby interfering with immunoblot analysis, the control MARK3 immunoblot blot in cell lysate was performed using the parental HeLa cell line that does not express GFP-TAP-14-3-3 ζ . The upper band in 14-3-3 blots of the TAP-eluate represents exogenously expressed 14-3-3 ζ and the lower doublet represents co-purified endogenous 14-3-3 ϵ and 14-3-3 ζ . The results are representative of three separate experiments.



from the different HeLa cell lines were incubated with 14-3-3 ζ conjugated to Sepharose, and immunoblot analysis of 14-3-3-associated proteins revealed that QSK (Fig. 2C) and SIK (Fig. 2D) were associated with 14-3-3 ζ derived from HeLa cells expressing wild-type LKB1, but not from LKB1-deficient control cells or cells expressing kinase-inactive LKB1. Control experiments showed that QSK, SIK and 14-3-3 isoforms were expressed at similar levels in control and LKB1-expressing HeLa cells and that, as expected, QSK and SIK were active only in HeLa cells expressing wild-type LKB1.

To further explore these observations, we generated HeLa lines that stably express GFP-TAP-14-3-3 ζ in the presence or absence of LKB1. QSK and SIK were associated with purified TAP-14-3-3 ζ in the HeLa cell line expressing wild-type LKB1, but not in LKB1-lacking cells (Fig. 2E).

In contrast to QSK and SIK, MARK3 was associated with 14-3-3-Sepharose in cell extracts derived from both LKB1-deficient HeLa cells and HeLa cells expressing wild-type LKB1 (Fig. 2F), and interacted with 14-3-3 ζ in both LKB1-

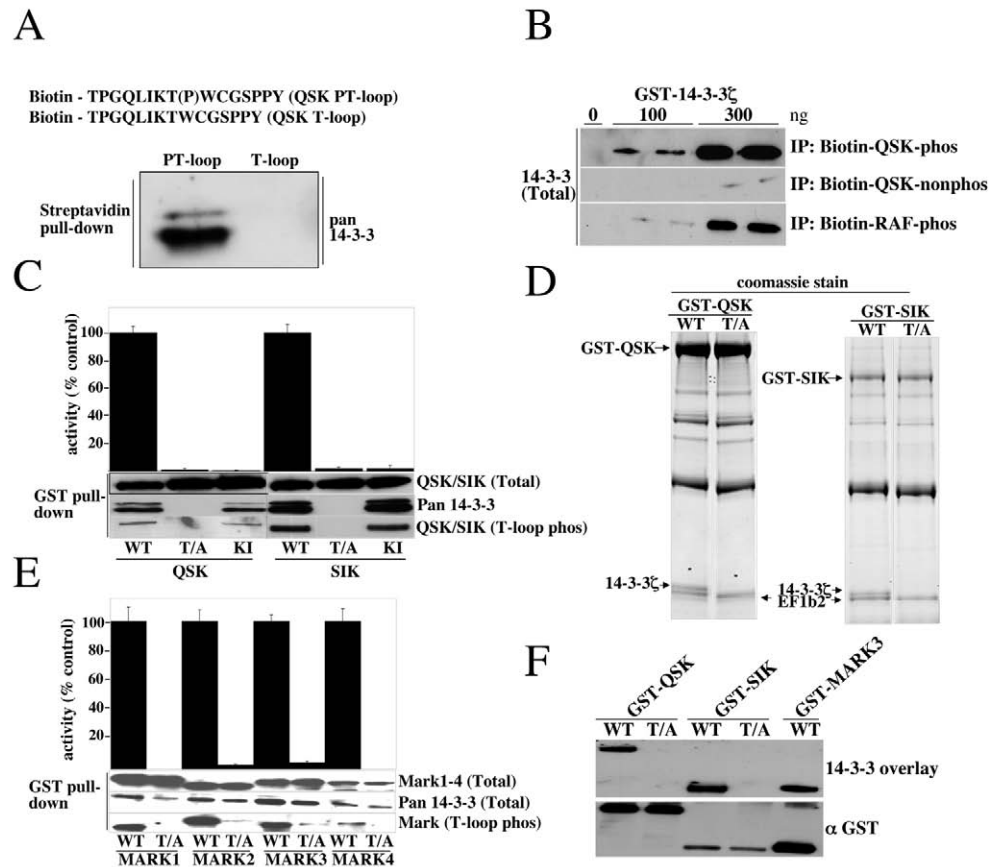
deficient and LKB1-expressing HeLa cells (Fig. 2E). The greater association of MARK3 with GFP-TAP-14-3-3 ζ in the LKB1-expressing cells is likely to be due to the increased expression of MARK3 in these cells (Fig. 2E).

Evidence that 14-3-3 binds to the phosphorylated T-loop of QSK and SIK

The finding that binding of 14-3-3 to QSK and SIK was dependent upon LKB1 could be explained if 14-3-3 interacted with the phosphorylated T-loop residue of these enzymes. To address this, we incubated 293 cell lysates with biotinylated peptides encompassing the T-loop of QSK, in which the Thr residue phosphorylated by LKB1 was either phosphorylated or non-phosphorylated. Following isolation of the peptides from the cell extract using streptavidin-Sepharose, 14-3-3 was associated with the phosphorylated T-loop peptide, but not with the non-phosphorylated T-loop peptide (Fig. 3A). We also tested the ability of recombinant 14-3-3 ζ to interact with these

Fig. 3. Binding of 14-3-3 to the phosphorylated T-loop of QSK and SIK. (A) 293 cell lysates were

incubated with the indicated N-terminal biotinylated peptides encompassing the T-loop of QSK. The peptides were affinity purified on streptavidin-Sepharose and immunoblotted with an antibody recognizing 14-3-3 isoforms. The results are representative of at least two separate experiments performed in duplicate. (B) 1 μ g of the indicated biotinylated peptides was conjugated to streptavidin-Sepharose and incubated with indicated amounts of GST-14-3-3 ζ . Following washing, the beads were subjected to immunoblot analysis with a 14-3-3 antibody. The RAF-phospho peptide LSQRQRSTS(P)TPNVHVMV binds 14-3-3 with high affinity (Muslin et al., 1996). (C,E) 293 cells were transfected with constructs encoding GST fusion proteins of wild-type (WT), T-loop mutant (T/A) or kinase-inactive (KI) mutants of the indicated AMPK-related kinases. Thirty-six hours post-transfection, the AMPK-related kinases were affinity purified from the cell lysates using glutathione-Sepharose. Similar amounts of the purified GST-fusion proteins were assayed for AMARA peptide kinase activity (activity) or subjected to immunoblot analysis (GST-pull-down). The QSK, SIK and MARK isoform levels were assessed using anti-GST antibodies. The kinase activities are presented as the mean \pm s.e.m. for triplicate samples relative to the activity observed for the wild-type kinase (100% activity). The results are representative of at least two separate experiments. (D) Equal amounts of wild-type and T-loop mutant of QSK and SIK GST fusion proteins isolated from 293 cells, as described in panel C, were electrophoresed on a polyacrylamide gel and the protein bands visualized by colloidal Coomassie Blue staining. The identity of the bands indicated with an arrow was determined by mass spectrometry. EF1b2 (elongation factor-1b2) is found as a contaminant in most preparations of GST-fusion derived from 293 cells. (F) 500 ng wild-type and T-loop mutant forms of GST-QSK and GST-SIK proteins, as well as wild-type GST-MARK3, were subjected to polyacrylamide gel electrophoresis, transferred to a nitrocellulose membrane and subjected to a 14-3-3 overlay assay (upper panel) as described in the Materials and Methods. 50 ng of each of the GST-fusion proteins was also subjected to immunoblot analysis with GST antibody (lower panel).



peptides. The phosphorylated QSK T-loop peptide interacted with 14-3-3 ζ to a markedly greater extent than did the non-phosphopeptide (Fig. 3B). Under the assay conditions employed, the phosphorylated QSK T-loop peptide interacted with 14-3-3 ζ to an extent similar to that of a well characterized 14-3-3 binding phosphopeptide encompassing Ser259 of the c-Raf protein kinase (Muslin et al., 1996).

We next expressed, in 293 cells, wild-type QSK or SIK as well as mutants of these enzymes that were catalytically inactive or in which the T-loop Thr phosphorylated by LKB1 was changed to Ala. The wild-type and catalytically inactive QSK and SIK associated with endogenous 14-3-3 proteins and were found to be phosphorylated at their T-loop residue, as revealed by immunoblotting with a phosphospecific antibody that recognizes this phosphorylation site (Fig. 3C). Analysis of a Coomassie-stained polyacrylamide gel of purified QSK and SIK indicated that a significant proportion of these enzymes were associated with 14-3-3 (Fig. 3D). By contrast, the QSK and SIK T-loop mutants failed to interact with 14-3-3 (Fig. 3C,D). All four MARK isoforms were associated with 14-3-3 when expressed in 293 cells (Fig. 3E). Consistent with the notion that LKB1 does not regulate binding of these enzymes to 14-3-3, mutation of the MARK T-loop Thr to Ala, although abolishing catalytic activity, did not affect binding to 14-3-3 (Fig. 3E).

14-3-3 binding to proteins has also been previously studied using a Far Western overlay approach, in which 14-3-3 binding to denatured proteins on a nitrocellulose membrane can be detected. Using this assay, we confirm that 14-3-3 isoforms were capable of interacting with wild-type QSK and SIK, but not with mutants of these enzymes in which the T-loop Thr phosphorylated by LKB1 was changed to Ala (Fig. 3F). This provides further evidence that 14-3-3 isoforms can interact directly with the phosphorylated T-loop of QSK and SIK.

14-3-3 activates QSK and SIK

We next investigated whether binding of 14-3-3 to QSK or SIK influenced catalytic activity. GST-SIK and GST-QSK were expressed in 293 cells, absorbed onto glutathione-Sepharose and, while still conjugated to the resin, incubated in the presence or absence

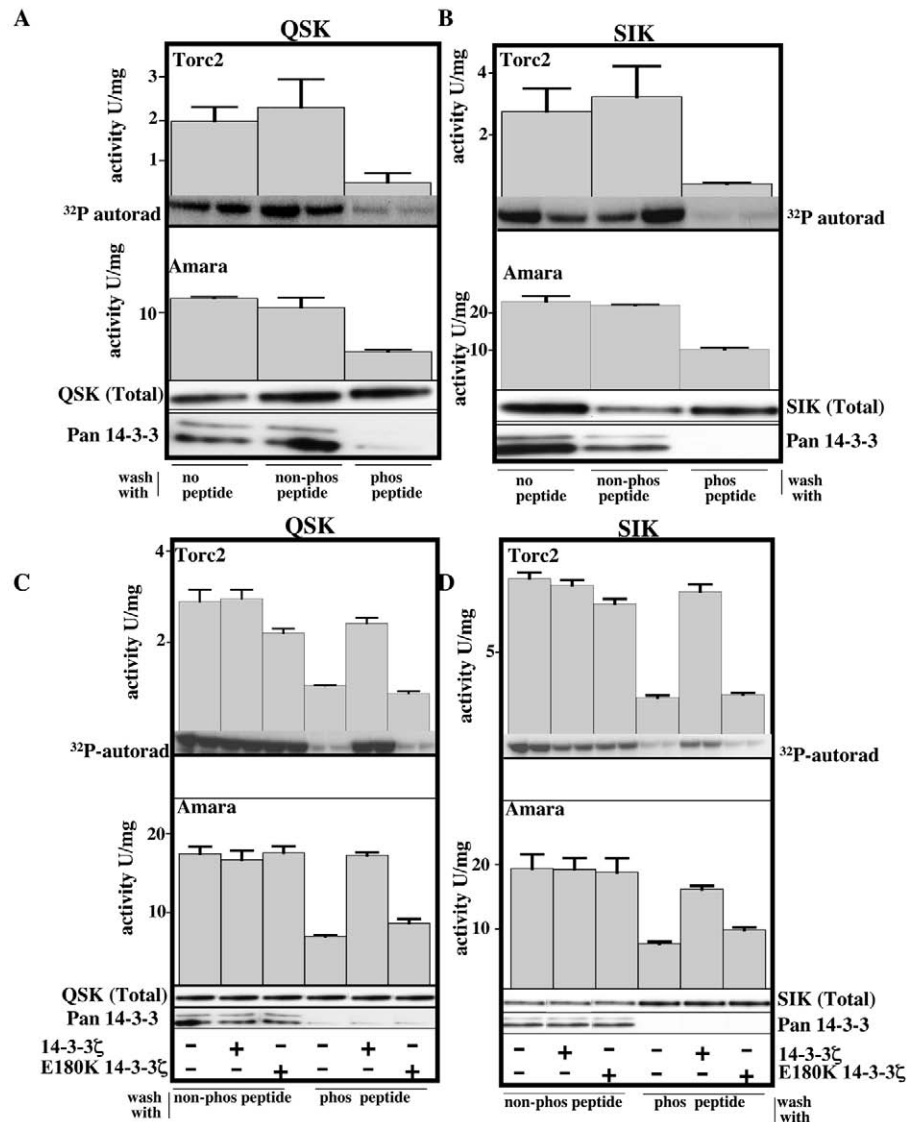


Fig. 4. Enhancement of QSK and SIK activity by 14-3-3 binding. 293 cells were transfected with constructs encoding GST-QSK (A,C) or GST-SIK (B,D). Thirty-six hours post-transfection, the GST-QSK or GST-SIK was absorbed onto glutathione-Sepharose and the beads were incubated with buffer containing no peptide, non-phosphorylated QSK T-loop peptide TPGQLIKTWCGSPPY (non-phos peptide) or phosphorylated QSK T-loop peptide TPGQLIKT(p)WCGSPPY (phos peptide). The beads were then washed in buffer A and GST-QSK or GST-SIK was eluted with glutathione. Similar amounts of the purified GST-QSK (A) or GST-SIK (C) were subjected to immunoblot analysis or assayed with either TORC2 protein substrate (upper panel), or the AMARA peptide (lower panel). The QSK and SIK levels were assessed in the immunoblot analysis using anti-GST antibodies. (C,D) GST-QSK (C) or GST-SIK (D) was also assayed using the TORC2 substrate (upper panel) or AMARA peptide (lower panel) in the presence (+) or absence (-) of wild-type GST-14-3-3 ζ or mutant GST-14-3-3 ζ [E180K]. In addition, the samples were immunoblotted with anti-GST antibodies, to ensure similar amounts of GST-QSK and GST-SIK were present in each assay, and with 14-3-3 antibody, to ensure removal of endogenously associated 14-3-3. The immunoblot analysis is representative of at least three separate experiments performed in duplicate. The kinase activities are presented as the mean \pm s.e.m. for triplicate samples and the results are representative of at least three separate experiments.

of the phosphorylated QSK-T-loop peptide or non-phosphorylated peptide. The phosphorylated but not the non-phosphorylated peptide dissociated 14-3-3 from GST-QSK

(Fig. 4A) or GST-SIK (Fig. 4B). We assayed QSK and SIK kinase activity using the CREB co-activator protein TORC2, a recently identified substrate for QIK (Screaton et al., 2004), which is also phosphorylated by QSK and SIK with an efficiency similar to that of QIK *in vitro* (A.K.A., unpublished). We also assayed QSK and SIK by employing the short AMARA peptide substrate (Lizcano et al., 2004). Dissociation of 14-3-3 from QSK (Fig. 4A) or SIK (Fig. 4B) resulted in a five- to sixfold reduction in activity when assayed with the TORC2 protein and a ~2.5-fold reduction in catalytic activity of these enzymes when assayed with the AMARA peptide substrate. Consistent with the reduction in activity resulting from a loss of 14-3-3 binding, addition of recombinant wild-type 14-3-3 ζ to GST-QSK (Fig. 4C) or GST-SIK (Fig. 4D) from which 14-3-3 had been dissociated, restored activity. By contrast, addition of 14-3-3 ζ [E180K] mutant, which is unable to interact with phosphopeptides (Chang and Rubin, 1997), failed to restore QSK or SIK activity.

14-3-3 influences QSK and SIK cellular localization

To examine whether binding of 14-3-3 to QSK and SIK could affect cellular localization, we expressed GFP-QSK and GFP-SIK in HeLa cells lacking LKB1, as well as in HeLa cells in which either wild-type or kinase-inactive LKB1 was stably expressed. QSK and SIK were expressed at similar levels in all cell lines (AKA, data not shown). In HeLa cells expressing wild-type LKB1, QSK (Fig. 5A, panel 1) or catalytically inactive QSK, which still binds 14-3-3, was localized in distinctive punctate structures within the cytosol (Fig. 5A, panel 2). By contrast, the T-loop QSK mutant, which is unable to bind 14-3-3, was localized more uniformly throughout the cytosol (Fig. 5A, panel 3), suggesting that punctate localization of QSK is dependent upon 14-3-3 binding. Consistent with this, in LKB1-deficient HeLa cells, wild-type and kinase-inactive QSK were uniformly localized in the cytosol rather than in punctate structures (Fig. 5A, panels 4-9).

Wild-type SIK or catalytically inactive SIK when expressed in HeLa cells expressing wild-type LKB1 were mostly localized within punctate structures inside the nucleus, but lower levels of SIK could be detected in the cytosol (Fig. 5B, panels 1,2). By contrast, wild-type or kinase-inactive SIK was exclusively localized within punctate structures of the nucleus and not

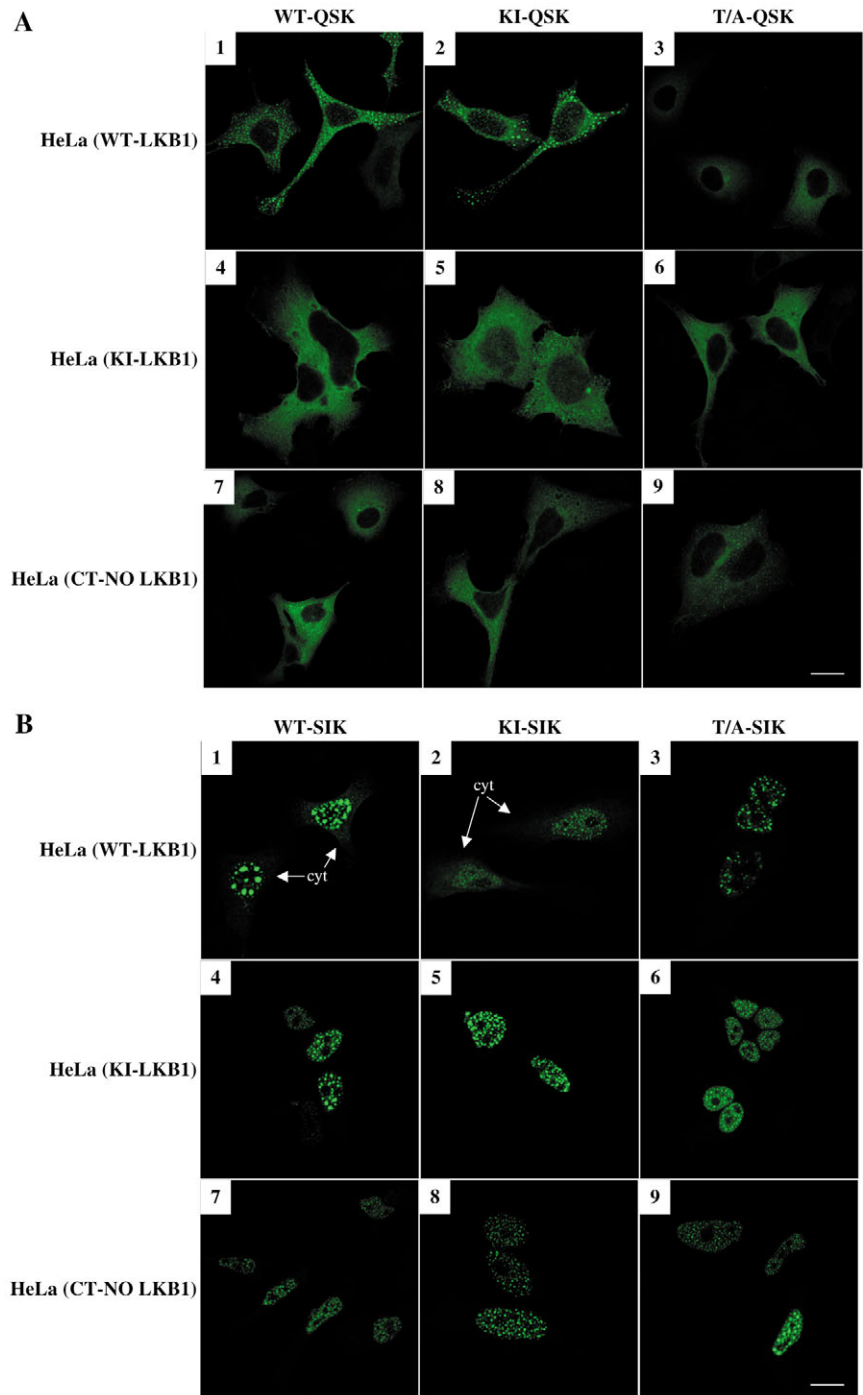


Fig. 5. 14-3-3 and LKB1 cooperate to regulate QSK and SIK localization. Control (CT) HeLa cells that lack LKB1 expression or HeLa cells that stably express wild-type (WT) or kinase-inactive (KI) LKB1 were transfected with the indicated constructs encoding the expression of GFP-QSK (A, panels 1-9) or GFP-SIK (B, panels 1-9). Twenty-four hours post-transfection the cells were fixed in 3% (v/v) paraformaldehyde and GFP localization was visualized directly by observing GFP fluorescence. The cells were viewed using a Zeiss LSM 510 META or Leica Sp2 AOBS confocal microscope. The cells shown are representative images obtained in three separate experiments. The low level of cytoplasmic SIK (cyt) is indicated. Bars, 10 μ m.

detected in the cytosol when expressed in LKB1-deficient HeLa cells (Fig. 5B, panels 4-9), indicating that binding of 14-

3-3 to SIK may be required for low levels of cytosolic localization of SIK. Consistent with this, the T-loop SIK mutant was localized exclusively within the nucleus when expressed in HeLa cells expressing wild-type LKB1 (Fig. 5B, panel 3).

Discussion

We have used the Tandem Affinity purification strategy to identify potential binding partners of the AMPK-related kinases in 293 cells. We have modified the TAP vector to include a GFP tag that facilitates the isolation of cell colonies expressing low levels of bait protein. We believe that generation of stable cell lines expressing low levels of bait proteins maximizes the proportion of the bait that is bound to endogenous binding partners, whose expression may be limiting. Thus, when MARK4 was expressed in 293 cells at high levels using a transient transfection approach we were able to detect the binding of MARK4 to 14-3-3 isoforms that are abundantly expressed in cells. However, under these conditions, we were unable to detect the interaction of MARK4 with USP9, which is likely to be expressed at lower levels than 14-3-3 isoforms (supplementary material Fig. S1). We also validated this approach by demonstrating that TAP-tagged AMPK α 1 was associated with its known AMPK β and AMPK γ regulatory subunits. We also identified several proteins that bind to some of the AMPK-related kinases and further work will be needed to investigate the physiological significance of these interactions.

Our previous work indicates that the AMPK-related kinases may be regulated in a distinct manner to that of AMPK, as none of the AMPK-related kinases were stimulated in cell lines or skeletal muscle by the AMP mimetic AICA-riboside or following treatments that elevate 5'-AMP (Lizcano et al., 2004; Sakamoto et al., 2004). The finding that the AMPK-related kinases, when purified from cells, are not associated with the AMPK β or AMPK γ regulatory subunits, which are required for the activation of AMPK by 5'-AMP, is likely to account for the inability of the AMPK-related kinases to be stimulated by 5'-AMP. Two pairs of CBS domains located within the AMPK γ subunit mediate the binding of 5'-AMP to AMPK. None of the proteins that were associated with the AMPK-related kinases possess predicted CBS domains, including NUA2, which was reported to be stimulated with AICAR (Lefebvre and Rosen, 2005) in hepatocarcinoma cells. We have previously shown in mouse embryonic fibroblast cells that NUA2 activity is not increased with AICAR (Lizcano et al., 2004). It may be worthwhile to investigate whether NUA2 could interact with AMPK γ or another CBS-domain-containing proteins in hepatocarcinoma cells.

14-3-3 proteins interact dynamically with many intracellular proteins, which exerts a widespread influence on diverse cellular processes. They operate by binding to specific phosphorylated residues on target proteins. In *C. elegans*, the 14-3-3 protein, termed Par-5, was originally identified as a gene that played a crucial role in the early events leading to polarization of the zygote (Morton et al., 2002). Par-5 was also required for the asymmetric cortical localization of Par-1/MARK to the posterior of the embryo, as well as locating the other polarity regulators, Par-3 and Par-6/PKC ζ , to the cell anterior (Morton et al., 2002). Work performed in *Drosophila*

(Benton et al., 2002) and in mammalian cells (Brajenovic et al., 2003), also indicated that the Par-1/MARK enzymes interacted directly with 14-3-3 isoforms. Recent studies suggest that phosphorylation of Par-1/MARK by the Par-6/PKC ζ kinase, at residue(s) lying C-terminal to the catalytic domain, induced a relocalization of Par-1/MARK from the plasma membrane and enhanced the binding of 14-3-3 to Par-1/MARK (Hurov et al., 2004; Kusakabe and Nishida, 2004; Suzuki et al., 2004a). Consistent with the 14-3-3 binding site(s) being located C-terminal to the catalytic domain, we observe that 14-3-3 isoforms bound to MARK3 in LKB1-deficient cells (Fig. 2F) and mutation of the T-loop Thr phosphorylated by LKB1 did not affect the ability of any MARK isoform to bind 14-3-3 (Fig. 3E). By contrast, binding of 14-3-3 to QSK and SIK was mediated by LKB1, as QSK and SIK failed to bind 14-3-3 in LKB1-deficient cells or skeletal muscle (Fig. 2). Moreover, mutation of the T-loop LKB1 phosphorylation site on QSK and SIK abolished 14-3-3 binding (Fig. 3C,F). The T-loops of QSK and SIK do not conform to the classical 14-3-3 binding motif (Mackintosh, 2004), but the finding that 14-3-3 isoforms expressed in cell lysates (Fig. 3A) or recombinant 14-3-3 ζ (Fig. 3B) could interact directly with a phosphorylated (but not non-phosphorylated) peptide encompassing the T-loop of QSK (Fig. 3A) indicates that this motif has the intrinsic ability to bind 14-3-3.

The binding of 14-3-3 to many proteins, including Par-1/MARK (Hurov et al., 2004; Kusakabe and Nishida, 2004) and TORC2 (Screaton et al., 2004), serves to localize these proteins in the cell cytosol. Our results also show that the binding of 14-3-3 isoforms to SIK and QSK plays a role in regulating the localization of these enzymes. In the case of SIK, binding to 14-3-3 induces a moderate redistribution of SIK from the nucleus to the cytosol (Fig. 5B) whereas, for QSK, interaction with 14-3-3 results in localization within punctate structures in the cytosol (Fig. 5A). Further work is required to characterize the punctate structures that QSK and SIK interact with and the mechanism by which 14-3-3 anchors QSK to punctate structures in the cytosol and localizes SIK in the cytoplasm. It would also be important to develop sensitive antibodies to study the localization of endogenously expressed QSK and SIK in wild-type and LKB1-deficient cell lines to ensure that the localization patterns are similar to those observed in the overexpressed studies.

Most interestingly, our results suggest that 14-3-3 binding to QSK and SIK enhances their catalytic activity (Fig. 4). As the T-loop of a kinase is a key motif in controlling intrinsic catalytic activity, binding of 14-3-3 to this region of QSK and SIK could induce a structural change that stabilizes these enzymes in an active conformation. Moreover, the effect of 14-3-3 binding on catalytic activity is more pronounced using the TORC2 protein substrate than the AMARA peptide substrate (Fig. 4). It has previously been reported that phosphorylation of TORC2 at Ser171 by the QIK AMPK-related kinase enabled TORC2 to bind 14-3-3 (Screaton et al., 2004). An intriguing possibility is that binding of QSK and SIK to 14-3-3 enhances the ability of QSK/SIK to interact with and phosphorylate 14-3-3-binding substrates such as TORC2. We found that QSK and SIK phosphorylated TORC2 at Ser171 as well as at least two additional residues, namely Ser70 and Ser348 (supplementary material Fig. S2). Dissociation of 14-3-3 from QSK and SIK reduced the extent of phosphorylation of Ser70,

Ser171 and Ser348 to a similar extent for each site (supplementary material Fig. S2), indicating that the presence of 14-3-3 does not influence the ability of QSK/SIK to phosphorylate specific residues on TORC2. It is also possible that the greater stimulation of QSK and SIK activity towards the TORC2 substrate than the AMARA peptide (Fig. 4), results from 14-3-3 ζ binding directly to TORC2 and converting it into a better substrate for QSK/SIK. It is unlikely that 14-3-3 would bind to the short AMARA peptide, and thus the ability of 14-3-3 ζ to stimulate of QSK and SIK AMARA peptide kinase activity is likely to result from the direct binding of 14-3-3 ζ to QSK/SIK.

In conclusion, we demonstrate that catalytic activity and localization of QSK and SIK are regulated by 14-3-3 binding to the T-loop of these enzymes following their phosphorylation by LKB1. To our knowledge, this is the first report of 14-3-3 binding to the T-loop of a protein kinase and directly influencing its catalytic activity. This represents a novel mechanism by which 14-3-3 can regulate biological function. 14-3-3 isoforms are dimers that possess two substrate-binding pockets per dimer (reviewed by Mackintosh, 2004). It is possible that if QSK/SIK occupied only one of the binding sites on the 14-3-3 dimer, then the other site might be available for the recruitment of a substrate of QSK/SIK. In this way, 14-3-3 isoforms could function as a scaffolding complex to facilitate the interaction of QSK/SIK with their 14-3-3-binding substrates. It is likely that many of the substrates of QSK/SIK, as well as other AMPK-related kinases, comprise 14-3-3-binding proteins and/or are converted to 14-3-3 binding proteins following their phosphorylation, a feature that could be exploited to identify substrates for these enzymes.

We thank Kei Sakamoto for providing the LKB1-deficient muscle extracts, Carol MacKintosh for helpful advice, Mark Peggie for cloning and generation of expression constructs for 14-3-3 ζ and TORC2, Agnieszka Kieloch for tissue culture, Rosie Clarke for FACS analysis, Grahame Hardie for the AMPK α 1 cDNA, the Sequencing Service (School of Life Sciences, University of Dundee, UK) for DNA sequencing, the Post Genomics and Molecular Interactions Centre for Mass Spectrometry facilities (School of Life Sciences, University of Dundee) and the protein production and antibody purification teams [Division of Signal Transduction Therapy (DSTT), University of Dundee] co-ordinated by Hilary McLauchlan and James Hastie for expression and purification of antibodies and the TORC2 protein. A.K.A. is supported by a Moffat Charitable Trust studentship and O.G. is supported by a Wenner-Gren Foundation fellowship. We thank the Association for International Cancer Research, Diabetes UK, the Medical Research Council, the Moffat Charitable Trust and the pharmaceutical companies supporting the Division of Signal Transduction Therapy Unit (AstraZeneca, Boehringer-Ingelheim, GlaxoSmithKline, Merck & Co., Merck KgaA and Pfizer) for financial support.

References

- Baas, A. F., Boudeau, J., Sapkota, G. P., Smit, L., Medema, R., Morrice, N. A., Alessi, D. R. and Clevers, H. C. (2003). Activation of the tumour suppressor kinase LKB1 by the STE20-like pseudokinase STRAD. *EMBO J.* **22**, 3062-3072.
- Baas, A. F., Smit, L. and Clevers, H. (2004). LKB1 tumor suppressor protein: PARTaker in cell polarity. *Trends Cell. Biol.* **14**, 312-319.
- Benton, R., Palacios, I. M. and St Johnston, D. (2002). Drosophila 14-3-3/PAR-5 is an essential mediator of PAR-1 function in axis formation. *Dev. Cell* **3**, 659-671.
- Bettencourt-Dias, M., Giet, R., Sinka, R., Mazumdar, A., Lock, W. G., Balloux, F., Zafiroopoulos, P. J., Yamaguchi, S., Winter, S., Carthew, R. W. et al. (2004). Genome-wide survey of protein kinases required for cell cycle progression. *Nature* **432**, 980-987.
- Boudeau, J., Baas, A. F., Deak, M., Morrice, N. A., Kieloch, A., Schutkowski, M., Prescott, A. R., Clevers, H. C. and Alessi, D. R. (2003). MO25alpha/beta interact with STRADalpha/beta enhancing their ability to bind, activate and localize LKB1 in the cytoplasm. *EMBO J.* **22**, 5102-5114.
- Brajenovic, M., Joberty, G., Kuster, B., Bouwmeester, T. and Drewes, G. (2003). Comprehensive proteomic analysis of human Par protein complexes reveals an interconnected protein network. *J. Biol. Chem.* **279**, 12804-12811.
- Campbell, D. G. and Morrice, N. A. (2002). Identification of protein phosphorylation sites by a combination of mass spectrometry and solid phase edman sequencing. *J. Biomol. Techn.* **13**, 121-132.
- Chang, H. C. and Rubin, G. M. (1997). 14-3-3 epsilon positively regulates Ras-mediated signaling in Drosophila. *Genes Dev.* **11**, 1132-1139.
- Corradetti, M. N., Inoki, K., Bardeesy, N., DePinho, R. A. and Guan, K. L. (2004). Regulation of the TSC pathway by LKB1: evidence of a molecular link between tuberous sclerosis complex and Peutz-Jeghers syndrome. *Genes Dev.* **18**, 1533-1538.
- Drewes, G., Ebneith, A., Preuss, U., Mandelkow, E. M. and Mandelkow, E. (1997). MARK, a novel family of protein kinases that phosphorylate microtubule-associated proteins and trigger microtubule disruption. *Cell* **89**, 297-308.
- Durocher, Y., Perret, S. and Kamen, A. (2002). High-level and high-throughput recombinant protein production by transient transfection of suspension-growing human 293-EBNA1 cells. *Nucleic Acids Res.* **30**, E9.
- Feldman, J. D., Vician, L., Crispino, M., Hoe, W., Baudry, M. and Herschman, H. R. (2000). The salt-inducible kinase, SIK, is induced by depolarization in brain. *J. Neurochem.* **74**, 2227-2238.
- Guo, S. and Kemphues, K. J. (1995). par-1, a gene required for establishing polarity in *C. elegans* embryos, encodes a putative Ser/Thr kinase that is asymmetrically distributed. *Cell* **81**, 611-620.
- Hardie, D. G. (2004). The AMP-activated protein kinase pathway – new players upstream and downstream. *J. Cell Sci.* **117**, 5479-5487.
- Hawley, S. A., Boudeau, J., Reid, J. L., Mustard, K. J., Udd, L., Makela, T. P., Alessi, D. R. and Hardie, D. G. (2003). Complexes between the LKB1 tumor suppressor, STRADalpha/beta and MO25alpha/beta are upstream kinases in the AMP-activated protein kinase cascade. *J. Biol.* **2**, 28.
- Hemminki, A., Markie, D., Tomlinson, I., Avizienyte, E., Roth, S., Loukola, A., Bignell, G., Warren, W., Aminoff, M., Hoglund, P. et al. (1998). A serine/threonine kinase gene defective in Peutz-Jeghers syndrome. *Nature* **391**, 184-187.
- Horike, N., Takemori, H., Katoh, Y., Doi, J., Min, L., Asano, T., Sun, X. J., Yamamoto, H., Kasayama, S., Muraoka, M. et al. (2003). Adipose-specific expression, phosphorylation of Ser794 in insulin receptor substrate-1, and activation in diabetic animals of salt-inducible kinase-2. *J. Biol. Chem.* **278**, 18440-18447.
- Hurov, J. B., Watkins, J. L. and Piwnicka-Worms, H. (2004). Atypical PKC phosphorylates PAR-1 kinases to regulate localization and activity. *Curr. Biol.* **14**, 736-741.
- Jaleel, M., McBride, A., Lizcano, J. M., Deak, M., Toth, R., Morrice, N. A. and Alessi, D. R. (2005). Identification of the sucrose non-fermenting related kinase SNRK, as a novel LKB1 substrate. *FEBS Lett.* **579**, 1417-1423.
- Jenne, D. E., Reimann, H., Nezu, J., Friedel, W., Loff, S., Jeschke, R., Muller, O., Back, W. and Zimmer, M. (1998). Peutz-Jeghers syndrome is caused by mutations in a novel serine threonine kinase. *Nat. Genet.* **18**, 38-43.
- Jones, R. G., Plas, D. R., Kubek, S., Buzzai, M., Mu, J., Xu, Y., Birnbaum, M. J. and Thompson, C. B. (2005). AMP-activated protein kinase induces a p53-dependent metabolic checkpoint. *Mol. Cell* **18**, 283-293.
- Kishi, M., Pan, Y. A., Crump, J. G. and Sanes, J. R. (2005). Mammalian SAD kinases are required for neuronal polarization. *Science* **307**, 929-932.
- Kusakabe, M. and Nishida, E. (2004). The polarity-inducing kinase Par-1 controls *Xenopus* gastrulation in cooperation with 14-3-3 and aPKC. *EMBO J.* **23**, 4190-4201.
- Lefebvre, D. L. and Rosen, C. F. (2005). Regulation of SNARK activity in response to cellular stresses. *Biochim. Biophys. Acta* **1724**, 71-85.
- Lefebvre, D. L., Bai, Y., Shahmoly, N., Sharma, M., Poon, R., Drucker, D. J. and Rosen, C. F. (2001). Identification and characterization of a novel sucrose-non-fermenting protein kinase/AMP-activated protein kinase-related protein kinase, SNARK. *Biochem. J.* **355**, 297-305.
- Legembre, P., Schickel, R., Barnhart, B. C. and Peter, M. E. (2004).

- Identification of SNF1/AMP kinase-related kinase as an NF-kappaB-regulated anti-apoptotic kinase involved in CD95-induced motility and invasiveness. *J. Biol. Chem.* **279**, 46742-46747.
- Lizzano, J. M., Goransson, O., Toth, R., Deak, M., Morrice, N. A., Boudeau, J., Hawley, S. A., Udd, L., Makela, T. P., Hardie, D. G. et al.** (2004). LKB1 is a master kinase that activates 13 kinases of the AMPK subfamily, including MARK/PAR-1. *EMBO J.* **23**, 833-843.
- Mackintosh, C.** (2004). Dynamic interactions between 14-3-3 proteins and phosphoproteins regulate diverse cellular processes. *Biochem. J.* **381**, 329-342.
- Moorhead, G., Douglas, P., Morrice, N., Scarabel, M., Aitken, A. and MacKintosh, C.** (1996). Phosphorylated nitrate reductase from spinach leaves is inhibited by 14-3-3 proteins and activated by fusicoccin. *Curr. Biol.* **6**, 1104-1113.
- Morton, D. G., Shakes, D. C., Nugent, S., Dichoso, D., Wang, W., Golden, A. and Kempthues, K. J.** (2002). The *Caenorhabditis elegans* par-5 gene encodes a 14-3-3 protein required for cellular asymmetry in the early embryo. *Dev. Biol.* **241**, 47-58.
- Muslin, A. J., Tanner, J. W., Allen, P. M. and Shaw, A. S.** (1996). Interaction of 14-3-3 with signaling proteins is mediated by the recognition of phosphoserine. *Cell* **84**, 889-897.
- Nishimura, I., Yang, Y. and Lu, B.** (2004). PAR-1 kinase plays an initiator role in a temporally ordered phosphorylation process that confers tau toxicity in *Drosophila*. *Cell* **116**, 671-682.
- Perkins, D. N., Pappin, D. J., Creasy, D. M. and Cottrell, J. S.** (1999). Probability-based protein identification by searching sequence databases using mass spectrometry data. *Electrophoresis* **20**, 3551-3567.
- Puig, O., Caspary, F., Rigaut, G., Rutz, B., Bouveret, E., Bragado-Nilsson, E., Wilm, M. and Seraphin, B.** (2001). The tandem affinity purification (TAP) method: a general procedure of protein complex purification. *Methods* **24**, 218-229.
- Rigaut, G., Shevchenko, A., Rutz, B., Wilm, M., Mann, M. and Seraphin, B.** (1999). A generic protein purification method for protein complex characterization and proteome exploration. *Nat. Biotechnol.* **17**, 1030-1032.
- Sakamoto, K., Goransson, O., Hardie, D. G. and Alessi, D. R.** (2004). Activity of LKB1 and AMPK-related kinases in skeletal muscle; effects of contraction, phenformin and AICAR. *Am J. Physiol. Endocrinol. Metab.* **287**, E310-E317.
- Sakamoto, K., McCarthy, A., Smith, D., Green, K. A., Hardie, D. G., Ashworth, A. and Alessi, D. R.** (2005). Deficiency of LKB1 in skeletal muscle prevents AMPK activation and glucose uptake during contraction. *EMBO J.* **24**, 1810-1820.
- Sapkota, G. P., Deak, M., Kieloch, A., Morrice, N., Goodarzi, A. A., Smythe, C., Shiloh, Y., Lees-Miller, S. P. and Alessi, D. R.** (2002). Ionizing radiation induces ataxia telangiectasia mutated kinase (ATM)-mediated phosphorylation of LKB1/STK11 at Thr-366. *Biochem. J.* **368**, 507-516.
- Screaton, R. A., Conkright, M. D., Katoh, Y., Best, J. L., Canettieri, G., Jeffries, S., Guzman, E., Niessen, S., Yates, J. R., 3rd, Takemori, H. et al.** (2004). The CREB coactivator TORC2 functions as a calcium- and cAMP-sensitive coincidence detector. *Cell* **119**, 61-74.
- Shaw, R. J., Bardeesy, N., Manning, B. D., Lopez, L., Kosmatka, M., DePinho, R. A. and Cantley, L. C.** (2004a). The LKB1 tumor suppressor negatively regulates mTOR signaling. *Cancer Cell* **6**, 91-99.
- Shaw, R. J., Kosmatka, M., Bardeesy, N., Hurley, R. L., Witters, L. A., DePinho, R. A. and Cantley, L. C.** (2004b). The tumor suppressor LKB1 kinase directly activates AMP-activated kinase and regulates apoptosis in response to energy stress. *Proc. Natl. Acad. Sci. USA* **101**, 3329-3335.
- Shulman, J. M., Benton, R. and St Johnston, D.** (2000). The *Drosophila* homolog of *C. elegans* PAR-1 organizes the oocyte cytoskeleton and directs oskar mRNA localization to the posterior pole. *Cell* **101**, 377-388.
- Suzuki, A., Kusakai, G., Kishimoto, A., Lu, J., Ogura, T. and Esumi, H.** (2003a). ARK5 suppresses the cell death induced by nutrient starvation and death receptors via inhibition of caspase 8 activation, but not by chemotherapeutic agents or UV irradiation. *Oncogene* **22**, 6177-6182.
- Suzuki, A., Kusakai, G., Kishimoto, A., Lu, J., Ogura, T., Lavin, M. F. and Esumi, H.** (2003b). Identification of a novel protein kinase mediating Akt survival signaling to the ATM protein. *J. Biol. Chem.* **278**, 48-53.
- Suzuki, A., Hirata, M., Kamimura, K., Maniwa, R., Yamanaka, T., Mizuno, K., Kishikawa, M., Hirose, H., Amano, Y., Izumi, N. et al.** (2004a). aPKC acts upstream of PAR-1b in both the establishment and maintenance of mammalian epithelial polarity. *Curr. Biol.* **14**, 1425-1435.
- Suzuki, A., Kusakai, G., Kishimoto, A., Shimojo, Y., Miyamoto, S., Ogura, T., Ochiai, A. and Esumi, H.** (2004b). Regulation of caspase-6 and FLIP by the AMPK family member ARK5. *Oncogene* **23**, 7067-7075.
- Wang, Z., Takemori, H., Halder, S. K., Nonaka, Y. and Okamoto, M.** (1999). Cloning of a novel kinase (SIK) of the SNF1/AMPK family from high salt diet-treated rat adrenal. *FEBS Lett.* **453**, 135-139.
- Woods, A., Johnstone, S. R., Dickerson, K., Leiper, F. C., Fryer, L. G., Neumann, D., Schlattner, U., Wallimann, T., Carlson, M. and Carling, D.** (2003). LKB1 is the upstream kinase in the AMP-Activated protein kinase cascade. *Curr. Biol.* **13**, 2004-2008.
- Woods, Y. L., Rena, G., Morrice, N., Barthel, A., Becker, W., Guo, S., Unterman, T. G. and Cohen, P.** (2001). The kinase DYRK1A phosphorylates the transcription factor FKHR at Ser329 in vitro, a novel in vivo phosphorylation site. *Biochem. J.* **355**, 597-607.
- Yoshida, K., Yamada, M., Nishio, C., Konishi, A. and Hatanaka, H.** (2000). SNRK, a member of the SNF1 family, is related to low K(+)-induced apoptosis of cultured rat cerebellar granule neurons. *Brain Res.* **873**, 274-282.